Hindawi Publishing Corporation
Journal of Nanomaterials
Volume 2013, Article ID 639354, 9 pages
http://dx.doi.org/10.1155/2013/639354

Research Article

Influence of Metallic Molar Ratio on the Electron Spin Resonance and Thermal Diffusivity of Zn–Al Layered Double Hydroxide

Abdullah Ahmed Ali Ahmed,[1,2] Zainal Abidin Talib,[1] and Mohd Zobir Hussein[3]

[1] *Department of Physics, Faculty of Science, Universiti Putra Malaysia (UPM), 43400 Serdang, Selangor, Malaysia*
[2] *Department of Physics, Faculty of Applied Science, Thamar University, Thamar 87246, Yemen*
[3] *Advanced Materials and Nanotechnology Laboratory, Institute of Advanced Technology (ITMA), Universiti Putra Malaysia (UPM), 43400 Serdang, Selangor, Malaysia*

Correspondence should be addressed to Abdullah Ahmed Ali Ahmed; abdullah2803@gmail.com
and Zainal Abidin Talib; zainalat@science.upm.edu.my

Received 25 June 2013; Revised 6 August 2013; Accepted 7 August 2013

Academic Editor: Christian Brosseau

The coprecipitation method was used to prepare Zn–Al layered double hydroxide (Zn–Al–NO_3-LDH) at pH 7.5 and different Zn^{2+}/Al^{3+} molar ratios of 2, 3, 4, 5, and 6. The elemental, structural, and textural properties of prepared samples were studied. The crystallinity of prepared LDH nanostructure decreases as Zn^{2+}/Al^{3+} molar ratio increases. The electron spin resonance (ESR) spectroscopy of different LDH samples showed new ESR spectra. These spectra were produced due to the presence of different phases with formed LDH such as ZnO phase and $ZnAl_2O_4$ spinel. At low Zn^{2+}/Al^{3+} molar ratio, the ESR signals were produced from the presence of free nitrate anions in the LDH interlayer. Above $Zn^{2+}/Al^{3+} = 2$, the ESR signals were attributed to the existence of ZnO phase and $ZnAl_2O_4$ spinel in the samples. Because the nuclear magnetic moment of ^{67}Zn is lower than ^{27}Al, the increasing in Zn^{2+}/Al^{3+} molar ratio causes a reduction of the magnetic activity of $ZnAl_2O_4$ spinel. Thermal diffusivity versus *in situ* temperature showed nonlinear relation for different samples due to the changing in the water content of LDH as temperature increases. The dc conductivity of samples decreased as Zn^{2+}/Al^{3+} molar ratio.

1. Introduction

Layered double hydroxides (LDHs), also knownas hydrotalcite structure, are a family of lamellar solids. LDHs may be represented by the general formula $[M^{II}_{1-x}M^{III}_x(OH)_2]^{x+} \cdot [(A^{n-}_{x/n}) \cdot mH_2O]^{x-}$. M^{II} and M^{III} are divalent and trivalent cations, respectively, which are situated at the center of octahedral (OH^-) units of the brucite-like layers with charge-balancing anions (A^{n-}) in the hydrated interlayer regions. n is the charge of anions (A^{n-}) that lead to the electroneutrality of LDH. The value x is defined by $[M^{III}/(M^{II} + M^{III})]$, and m is the amount of LDH interlayer water molecules [1, 2]. The coprecipitation method is a common method to prepare the LDHs [1, 3, 4] and is done by the mixing of salts of divalent and trivalent cations under certain parameters (such as pH value, stirring, and cations molar ratio).

Electron spin resonance (ESR) spectroscopy is an important tool in research due to its ability to investigate several features of examined samples. The geometry and the arrangement components of intercalated guests into LDH interlayer could be identified using ESR spectroscopy [5, 6]. ESR has also been used to study the electronic structure of metallic centers of a mixed LDH and oxide material to explain its interaction with cations of LDH layers [7]. In a recent study, ESR has been used to investigate the isolation of the sebacate when this material was intercalated into LDH [8]. In our recent observation [9], ESR spectra have been used to explain the effect of temperature treatment on the nature of nitrate anions in LDH interlayer.

Thermal properties (including thermal diffusivity) of clays (soils, sands, LDHs, etc.) are very vital parameters in the heat transfer from or to buildings, in the distribution rate of electric cables and in the design of heating systems [10]. Thermal diffusivity of sands (Utah tar sands) has been measured [11] and had a range of 5×10^{-7}–9×10^{-7} $m^2\ s^{-1}$ over the temperature range of 27–147°C using a constant applied heat flux method. Thermal diffusivity of soils has been measured using the line heat source transient method [10] between the temperature –10°C and 35°C. The effect of moisture content up to 40% on diffusivity was also studied. Hinkel [12] has estimated thermal diffusivity of soils from two different regions which was between 1.5 and 2.1×10^{-7} $m^2\ s^{-1}$. In our recent paper [9], the effect of *in situ* temperatures in the range of 27–210°C on thermal diffusivity of Zn–Al–NO_3-LDH has been studied.

In this work, a series of Zn–Al–NO_3-LDH samples were prepared by the coprecipitation method at different Zn^{2+}/Al^{3+} molar ratios of (2, 3, 4, 5, and 6) and at constant pH value of 7.5. The structural and textural properties of samples were studied. The effect of Zn^{2+}/Al^{3+} molar ratios on ESR spectra and thermal diffusivity of Zn–Al–NO_3-LDHs were obtained.

2. Experimental

2.1. Materials and Preparation of Samples. The starting chemicals of zinc nitrate ($Zn(NO_3)_2{\cdot}6H_2O$) (Systerm, 98%), aluminum nitrate ($Al(NO_3)_3{\cdot}9H_2O$) (Hamburg Chemicals Co., 99.4%), and sodium hydroxide (NaOH) (Merck Co., 99%) were used without further purification. Deionized water was used as solvent throughout this study. The preparation of Zn–Al–NO_3-LDH precursors with starting value of molar ratio Zn^{2+}/Al^{3+} = 2, 3, 4, 5, and 6 has been carried out using coprecipitation method and has been presented elsewhere [13]. The samples were labeled as Zn*r*Al-LDH, where *r* represents the Zn^{2+}/Al^{3+} molar ratio.

2.2. Characterizations. Elemental analyses for Zn and Al were measured by inductively coupled plasma emission spectroscopy (ICP) (Perkin-Elmer, Optima 2000 DV) after dissolving the samples in hydrochloric acid. Powder X-ray diffraction (PXRD) patterns of the samples were recorded on a X-ray diffractometer (X'pert-PRO Panalytical) using CuK_α (λ = 1.54187 Å) at 40 kV and 30 mA. The surface areas and pore volumes of the samples were characterized using the nitrogen gas adsorption-desorption technique at 77 K using a Micromeritics ASAP 2000 instrument (Norcross, GA). Electron spin resonance (ESR) spectra were recorded using a JEOL ESR spectrometer (JES-FA200). Thermal diffusivity versus temperature was performed using NETZSCH model LFA 457 *MicroFlash*. The dielectric measurements of samples have been obtained using novocontrol high resolution dielectric analyzer.

3. Results and Discussion

3.1. Elemental Chemical Analysis. In this section, in addition to ICP analysis, we have used TGA data from our published paper [13] to calculate the chemical formulae of different samples. The chemical compositions of prepared Zn–Al–NO_3-LDH samples at Zn^{2+}/Al^{3+} molar ratio of 2, 3, 4, 5, and 6 are listed in Table 1. The experimental Zn^{2+}/Al^{3+} molar ratio is close to that in the starting solutions. As seen in Table 1, the formula considers that nitrate is the only compensating anion in the LDH interlayer region. Carbonate impurities do not take into account the possible presence in the interlayer gallery. These results are in good agreement with that reported by Rojas Delgado et al. [14].

3.2. Powder X-Ray Diffraction (PXRD) Study. Figure 1 exhibits the PXRD patterns of Zn–Al–NO_3-LDH precursors with Zn^{2+}/Al^{3+} molar ratio of 2, 3, 4, 5, and 6. The characteristic reflections of Zn–Al–NO_3-LDH samples show the different planes which are listed in Table 2. For the samples Zn4Al-LDH, Zn5Al-LDH, and Zn6Al-LDH, the PXRD patterns show the characteristic reflections of ZnO phase and the patterns of $ZnAl_2O_4$ spinel [15]. The decreasing of PXRD intensity of the LDH peaks was observed as the Zn^{2+}/Al^{3+} molar ratio increases. These changes are attributed to the formation of other phases (ZnO phase and $ZnAl_2O_4$ spinel) with low crystallinity. This caused the distortion of the hydroxide layers networks of the LDH crystal by the larger difference in ionic radii of Zn^{2+} and Al^{3+} [16]. Yan et al. have employed the density functional theory to study the influence of cations ratio on the host layer structure of Zn–Al-LDHs [17]. They have shown that the formation or bonding stability of the corresponding Zn*r*Al-LDH (*r*: molar ratio = 2, 3, 4, 5, and 6) clusters decreases with increasing the molar ratio (*r*). Another study has also demonstrated that the decreasing of Al^{3+} concentration in Zn–Al-LDH solution causes the decreasing of the crystallinity of LDH phase [18]. Our results are in good agreement with all of those literatures which exhibited significant increase in crystallinity of Zn*r*Al-LDH as Zn^{2+}/Al^{3+} molar ratio decreases.

3.3. N_2 Adsorption-Desorption Study. The pore size distribution of the prepared samples was studied using the Barrett-Joyner-Halenda (BJH) method from the desorption branch of the isotherms as shown in Table 2. The observation is supported by the analyses of the pore structure and surface area of the samples. Figure 2 shows the nitrogen adsorption-desorption isotherms of Zn–Al–NO_3-LDH prepared at different Zn^{2+}/Al^{3+} molar ratio. All the isotherms are generally Type III-like with a distinct H3 hysteretic loop in the range of 0.2–1.0 P/P_0. These results show the presence of macroporous materials (the volume of pores are greater than 0.05 μm) according to IUPAC classifications [19]. Results from Rojas Delgado et al. on the total layer specific area for Zn–Al–Cl-LDH [14] reflect an increase from 924 m^2/g (for Zn^{2+}/Al^{3+} molar ratio = 2.4) to 941 m^2/g (for Zn^{2+}/Al^{3+} molar ratio = 4.8). As seen in Table 2, the BET surface area increases from 0.12 to 8.34 m^2/g when Zn^{2+}/Al^{3+} molar ratio increases

Table 1: Elemental chemical analysis data and interlayer water content of Zn-Al-NO_3-LDH samples and their calculated formulae using ICP analysis.

Sample	% Zn	% Al	% H_2O[a]	$Zn^{2+}/Al^{3+}{}_{exp}$	Chemical formulae
Zn2Al-LDH	38.67	7.73	7.38	2.06	$Zn_{0.67}Al_{0.33}(OH)_2(NO_3)_{0.33}{\cdot}0.47H_2O$
Zn3Al-LDH	42.98	6.06	7.18	2.93	$Zn_{0.75}Al_{0.25}(OH)_2(NO_3)_{0.25}{\cdot}0.45H_2O$
Zn4Al-LDH	49.74	5.17	6.02	3.97	$Zn_{0.80}Al_{0.20}(OH)_2(NO_3)_{0.20}{\cdot}0.37H_2O$
Zn5Al-LDH	51.18	4.26	5.89	4.95	$Zn_{0.83}Al_{0.17}(OH)_2(NO_3)_{0.17}{\cdot}0.36H_2O$
Zn6Al-LDH	50.01	3.72	6.26	5.54	$Zn_{0.85}Al_{0.15}(OH)_2(NO_3)_{0.15}{\cdot}0.38H_2O$

[a]These results were obtained by TGA data from our work [13].

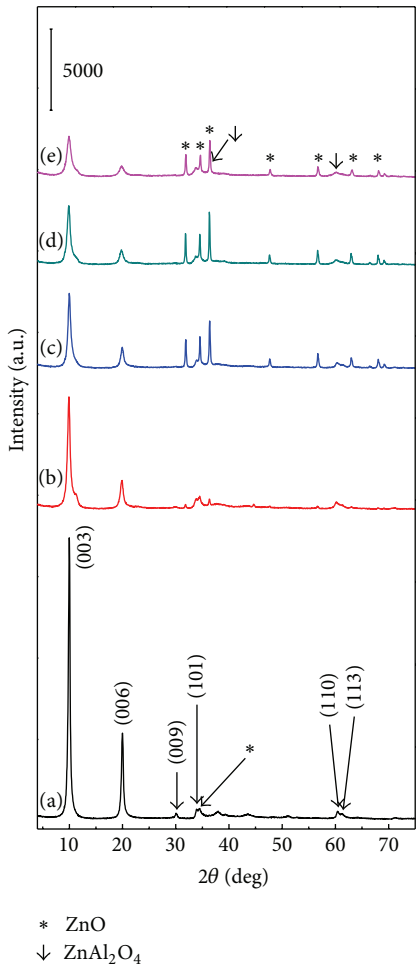

Figure 1: PXRD patterns of (a) Zn2Al-LDH, (b) Zn3Al-LDH, (c) Zn4Al-LDH, (d) Zn5Al-LDH, and (e) Zn6Al-LDH.

from 2 to 6 due to the increasing of electrostatic repulsion between adjacent trivalent metals in the layers [14, 20]. On the other hand, the BJH average pore diameter has the opposite behavior of BET surface area with the highest value of 18.86 μm at Zn^{2+}/Al^{3+} molar ratio of 2.

3.4. Electron Spin Resonance (ESR) Spectra. New ESR spectra of the LDH samples exhibit signal with different intensities and sharpness at room temperature as shown in Figure 3. For Zn2Al-LDH, a broad and weak signal with a g-factor = 2.01105 is observed, which is attributed to the interaction between nitrate anions from the interlayer region and a close aluminum nucleus ($I = 5/2$) from the LDH sheets. This signal is characteristic of NO_3^- ions with D_{3h} symmetry in the LDH interlayer [21]. As seen in our recent paper [13], the FT-IR results showed that the LDH interlayer NO_3^- anions existed with a D_{3h} symmetry. There is also a possibility that this signal is due to a weak interaction of the free electron of NO_3^- radical with the nuclear magnetic moment of protons of the water matrix in LDH interlayer [22]. Two signals with stronger intensity begin to appear for samples at Zn^{2+}/Al^{3+} molar ratio of 3 and above; the first one with a g-factor = 2.18870 is attributed to the formation of $ZnAl_2O_4$ spinel, while the second signal with a g-factor = 1.93337 is ascribed to the existence of ZnO phase in the samples.

In $ZnAl_2O_4$, the most probable centers that can be observed are the V centers (a hole trapped in a cation vacancy) and F^+ centers (an electron trapped in an anion vacancy) [23]. The signal of $ZnAl_2O_4$ is due to the presence of an interaction between the oxygen vacancies of $ZnAl_2O_4$ and the aluminium nucleus ($I = 5/2$). For the ZnO signal, the oxygen vacancies on the ZnO surface are responsible for the generation of the ESR signals. The Zn^+ ion, which has a $4s^1$ orbital, will also appear on the ZnO surface and produces a parametric signal [24].

As seen in Figure 4, the evolution of the normalized ESR intensity against Zn^{2+}/Al^{3+} molar ratio for ZnO phase and $ZnAl_2O_4$ spinel is plotted. The relative intensity of samples increases until Zn^{2+}/Al^{3+} molar ratio = 5 which has the highest ESR intensity for ZnO phase, and then it starts to decrease. For the $ZnAl_2O_4$ spinel, the highest ESR intensity was at Zn^{2+}/Al^{3+} molar ratio = 4. Aluminum and zinc cations in $ZnAl_2O_4$ have isotopes with nuclear spin of 5/2: ^{27}Al and ^{67}Zn. ^{27}Al is much more abundant (100%) than ^{67}Zn (4.11%), and its nuclear magnetic moment is higher (3.6385) than that of ^{67}Zn (0.8753) [25]. The increase in Zn^{2+}/Al^{3+} molar ratio causes a reducing of the magnetic activity of $ZnAl_2O_4$ because the nuclear magnetic moment of ^{67}Zn is lower than ^{27}Al. On the other hand, for ZnO phase, the magnetic activity increases which may be attributed to the increase in parametric of oxygen in the excess of Zn cations of LDH. The rapidly drop in the intensity of ZnO and stability of $ZnAl_2O_4$ may refer to the low crystallinity of whole system due to the distortion of the hydroxide layers networks of the LDH crystal as seen in PXRD results.

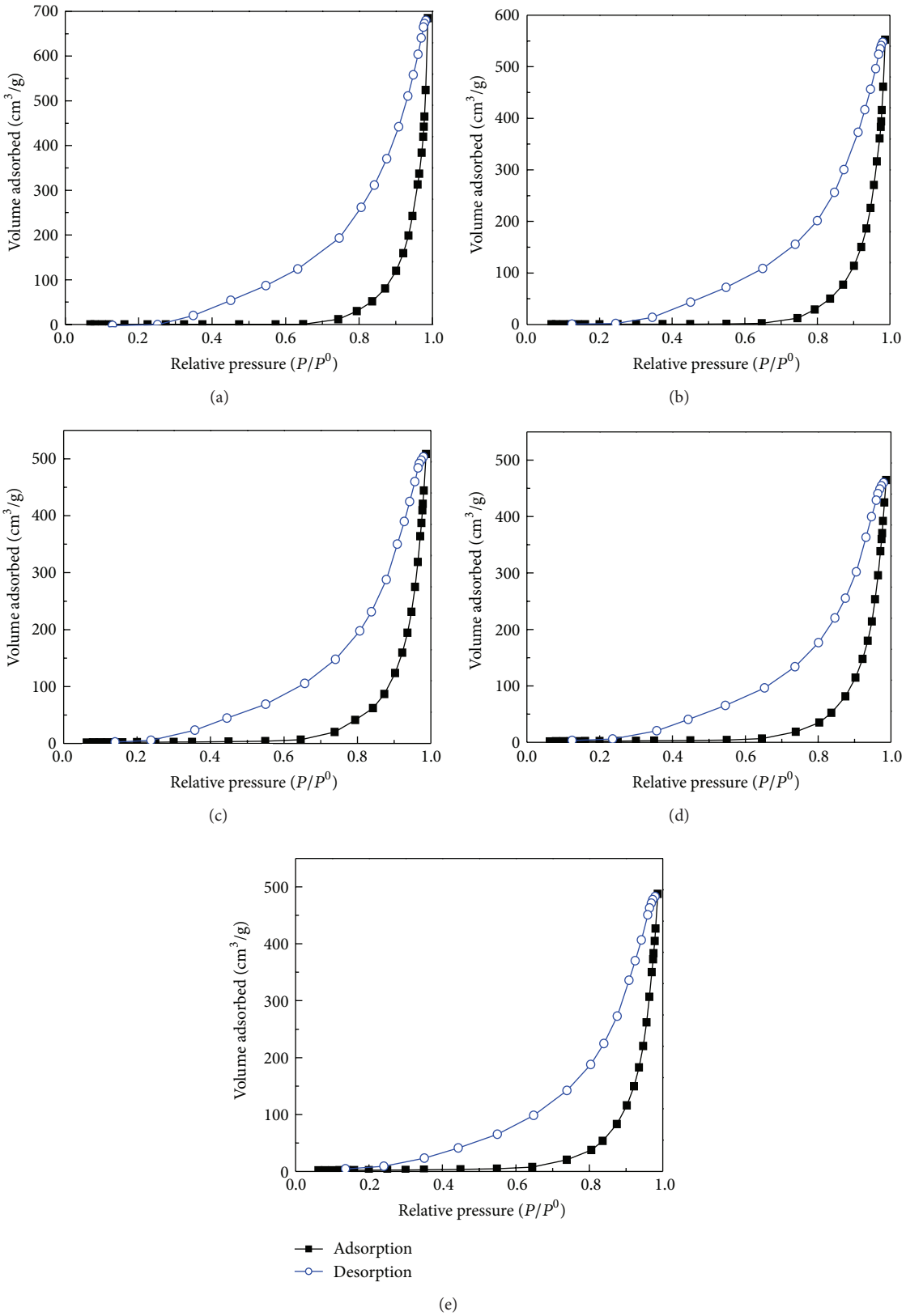

FIGURE 2: N_2 adsorption-desorption isotherms of (a) Zn2Al-LDH, (b) Zn3Al-LDH, (c) Zn4Al-LDH, (d) Zn5Al-LDH, and (e) Zn6Al-LDH.

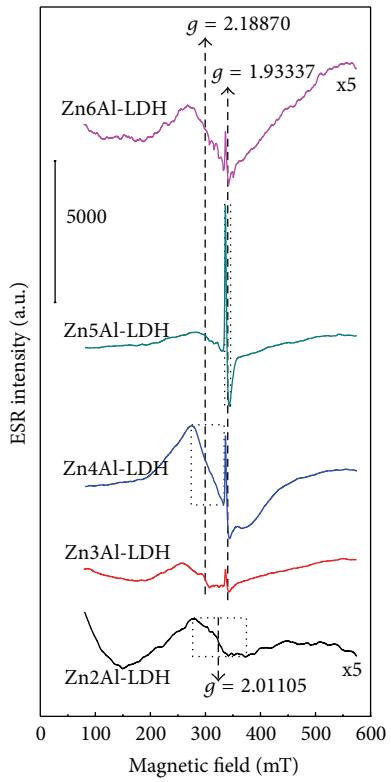

Figure 3: ESR spectra of Zn2Al-LDH, Zn3Al-LDH, Zn4Al-LDH, Zn5Al-LDH, and Zn6Al-LDH at room temperature.

3.5. Thermal Diffusivity. Thermal diffusivity (α) measures the ability of a material to conduct thermal energy relative to its ability to store thermal energy. The relation between thermal diffusivity (under transient conditions) and thermal conductivity (k) (under steady-state conditions) described the heat transport in materials using the following equation [26]:

$$\alpha = \frac{k}{\rho c_p}, \tag{1}$$

where c_p is the specific heat capacity and ρ is the density.

In this work, LFA-457 NETSCH equipment has been used to measure the thermal diffusivity. The setup consists of a laser source which radiates a short-time energy pulse that strikes the front of the cylindrical sample (diameter 10 mm and thick between 1 and 2 mm). The transient temperature at the opposite side, which increases over time, is measured by infrared detector triggered simultaneously with laser beam. The mathematical thermal model of the experiment is represented by differential equation whose solution of this equation can be expressed as

$$T'^{(L,t)} = \frac{T(L,t)}{T_{\max}} = 1 + 2\sum_{n=1}^{\infty}(-1)^n e^{-(n\pi)^2(\alpha t/L^2)}, \tag{2}$$

where L is the thickness of the sample and $T_{\max}$ is the highest temperature at the rear surface of sample. The mathematical

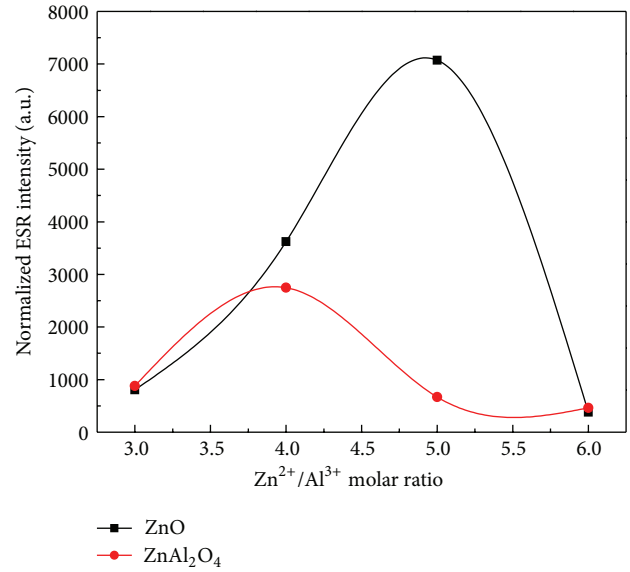

Figure 4: Variation of the normalized ESR intensity as a function of pH value of the prepared samples.

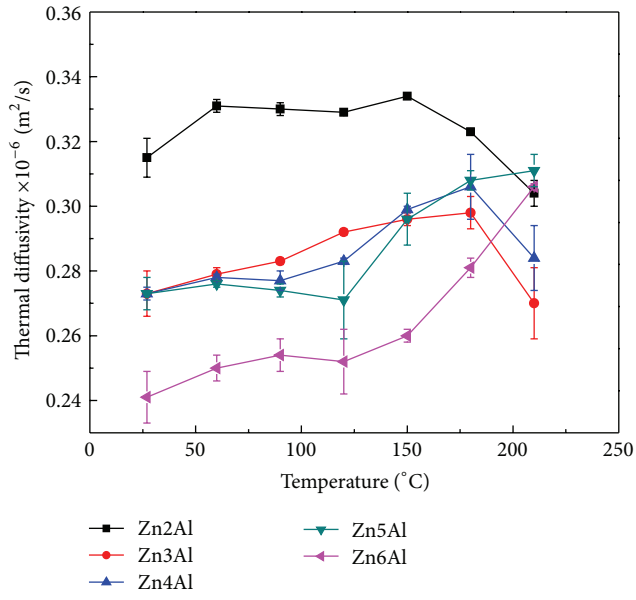

Figure 5: Thermal diffusivity versus temperature of Zn2Al-LDH, Zn3Al-LDH, Zn4Al-LDH, Zn5Al-LDH, and Zn6Al-LDH.

analysis of the temperature versus time plot by (2) enables one to determine the thermal diffusivity as the following [27]:

$$\alpha = \frac{1.388\ L^2}{t_{1/2}}, \tag{3}$$

where $t_{1/2}$ is the time corresponding to 50% of the increase in the temperature measured on the opposite surface of the sample.

Figure 5 shows a nonlinear relation of thermal diffusivity versus *in situ* temperatures for Zn–Al-LDH at different Zn^{2+}/Al^{3+} molar ratios. The values of thermal diffusivity

Table 2: Lattice parameters and surface properties of Zn–Al–NO_3-LDH samples.

Sample	d_{003} (nm)	d_{110} (nm)	a[a] (nm)	c[b] (nm)	D[c] (nm)	S_{BET}[d] (m^2/g)	V_p[e] (cm^3/g)	D_{BJH}[f] (μm)
Zn2Al-LDH	0.883	0.153	0.306	2,66	29.18	0.12	0.68	18.86
Zn3Al-LDH	0.889	0.154	0.308	2.67	23.16	2.04	0.61	1.17
Zn4Al-LDH	0.885	0.154	0.308	2.66	28.42	7.64	0.63	0.33
Zn5Al-LDH	0.891	0.154	0.308	2.68	17.61	7.74	0.57	0.30
Zn6Al-LDH	0.890	0.154	0.308	2.68	32.51	8.34	0.59	0.28

[a] $a = 2\ d_{110}$.
[b] c = average value calculated from (003) and (006) reflections.
[c] Average crystallite size in c direction value calculated from the values of (003) and (006) diffraction peaks using the Scherrer equation.
[d] Brunauer-Emmett-Teller (BET) surface area.
[e] Barret-Joyner-Halenda (BJH) pore volume.
[f] Barret-Joyner-Halenda (BJH) average pore diameter.

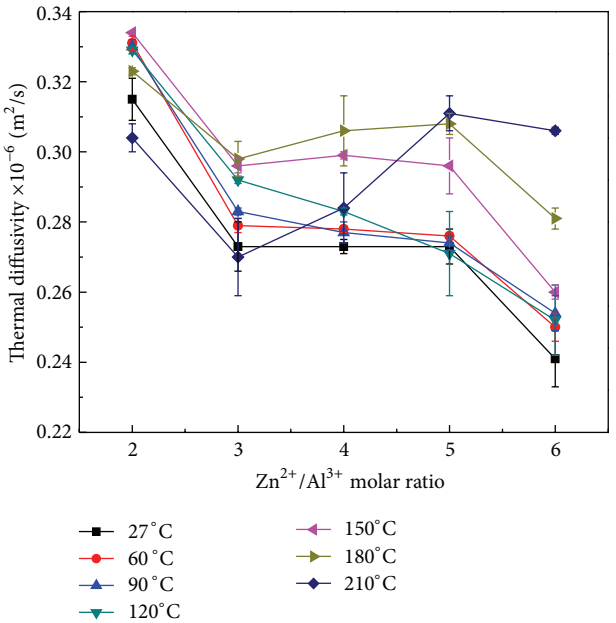

Figure 6: The thermal diffusivity as a function of Zn^{2+}/Al^{3+} molar ratio of LDH for several *in situ* temperatures.

Table 3: Values of dc conductivity σ_{dc}, preexponential factor A and the fractional exponent n for Zn–Al–NO_3-LDH samples.

Sample	$\sigma_{dc} \times 10^{-4}$ (S/cm)	A	n
Zn2Al-LDH	15.80	7.22×10^{-4}	0.07
Zn3Al-LDH	3.14	2.06×10^{-6}	0.41
Zn4Al-LDH	1.41	2.40×10^{-10}	0.99
Zn5Al-LDH	0.14	2.00×10^{-10}	0.99
Zn6Al-LDH	0.07	7.08×10^{-10}	0.89

for samples were found between 2.4 and 3.3 $\times 10^{-7}$ $m^2\ s^{-1}$ which are close to the values that have been reported [9, 28]. For Zn2Al-LDH, the thermal diffusivity is almost constant as temperature increases until around 150°C. Above 150°C, the values of thermal diffusivity drop rapidly as temperature increases because the water molecules start to release from LDH. The thermal diffusivity of this sample in this temperature range may be attributed to the high crystallinity of Zn2Al-LDH, and this sample is almost free from other phases as shown in PXRD results.

From TGA results [13], water molecules were completely removed and LDH starts to collapse at 180°C and above. For the samples Zn3Al-LDH, Zn4Al-LDH, Zn5Al-LDH, and Zn6Al-LDH, in general, the behavior of thermal diffusivity increases as *in situ* temperature increases until around 180°C and then drops rapidly as temperature increases. Thus thermal behavior in this range is strongly influenced by the water content in LDH [29]. Above 180°C, ZnO phase is purely responsible for the decrease in the thermal diffusivity [9].

Figure 6 shows a nonlinear relation of the thermal diffusivity as a function of Zn^{2+}/Al^{3+} molar ratio of LDH for all measured temperatures. The thermal diffusivity decreases as the molar ratio increases which can be attributed to the presence of ZnO and $ZnAl_2O_4$ phases. At temperature 210°C, the behavior is different due to the collapse of LDH structure [30, 31]. In addition to the decrease in the crystallinity as Zn^{2+}/Al^{3+} molar ratio increases, the presence of Zn–O and Al–O in an octahedral coordination state in LDH brucite-like sheet causes decreasing of thermal conductivity as temperature increases which may result from the random disorder phonon scattering induced by the Al deficient sites [32].

3.6. The Dc Conductivity. The dc conductivity or ionic conductivity (σ_{dc}) can be calculated using the Jonscher power law [33]:

$$\sigma_{ac}(\omega) = \sigma_{dc} + A\omega^n, \quad (4)$$

where A is the preexponential factor and the value of n is between 0 and 1 for this material. The equation (4) has been used to fit the experimental data of real part of conductivity $\sigma'(\omega)$ which were presented in the previous work [13] as shown in Figure 7. The solid line denotes the fit to power law expression of data, and the values (σ_{dc}, A, and n) can be achieved using Origin nonlinear curve fitting software and listed in Table 3. The disagreement in the fit curves with experimental data at low frequency was attributed to the polarization effect of the electrode.

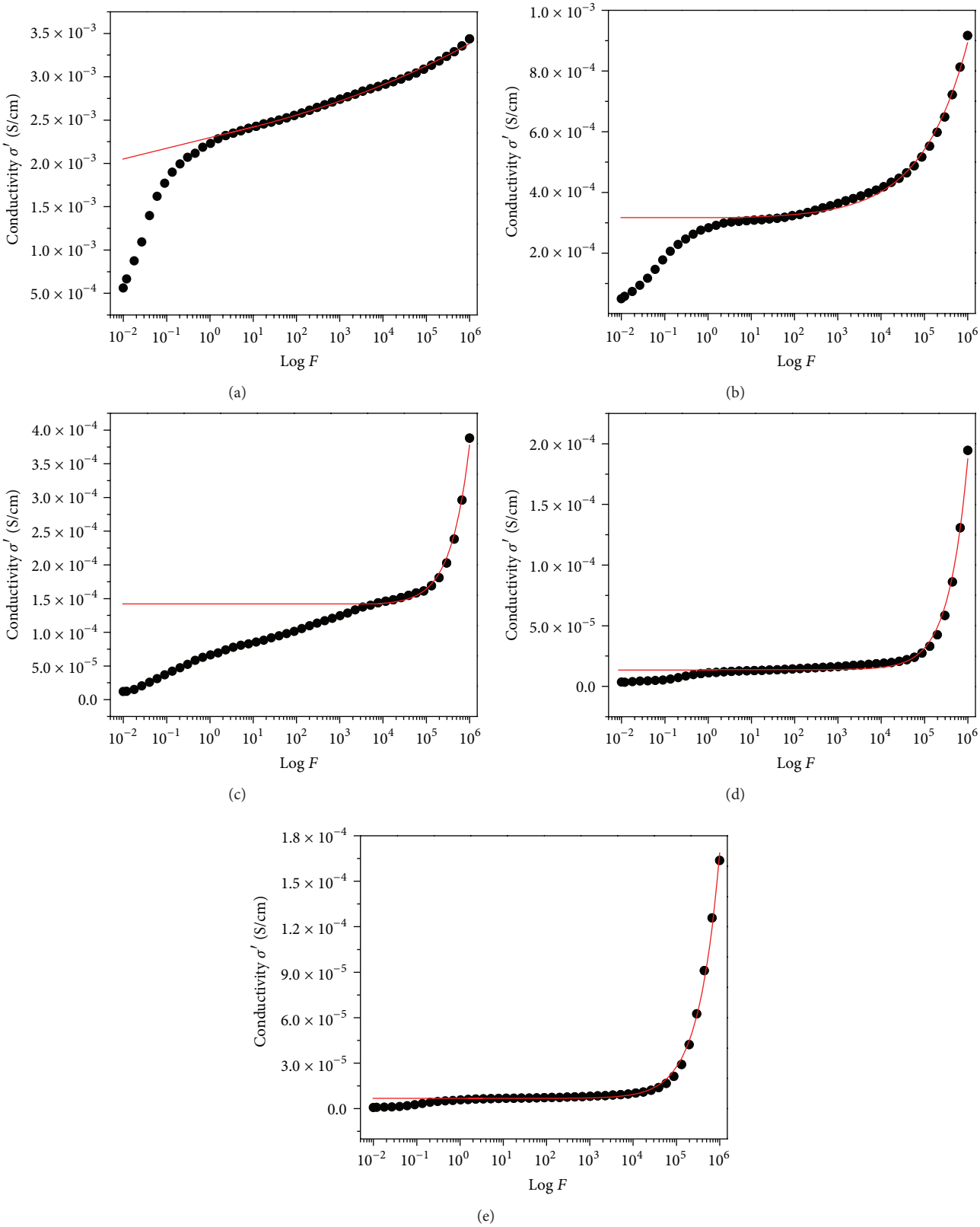

FIGURE 7: The fitting curves of the experimental data of σ' versus frequency for (a) Zn2Al-LDH, (b) Zn3Al-LDH, (c) Zn4Al-LDH, (d) Zn5Al-LDH, and (e) Zn6Al-LDH.

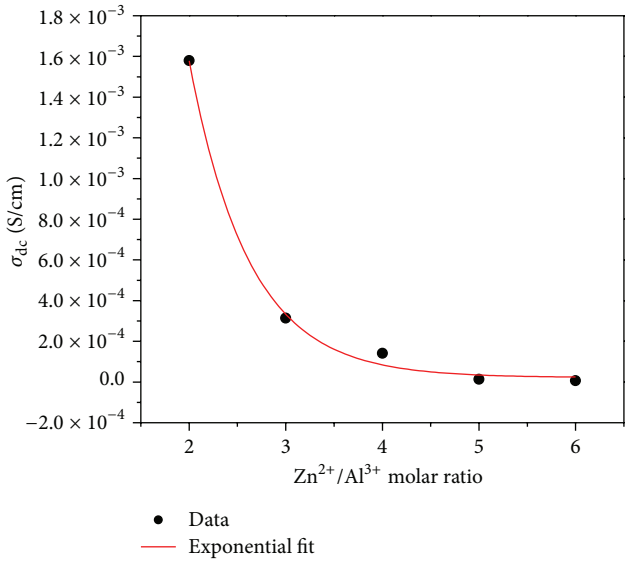

FIGURE 8: The variation of dc conductivity versus Zn/Al molar ratio.

The obtained σ_{dc} values from the fit curves for all samples were plotted against Zn^{2+}/Al^{3+} molar ratio as shown in Figure 8. This relation illustrated that dc conductivity decreased exponentially with the increase in the Zn^{2+}/Al^{3+} molar ratio of the prepared samples. This may suggest that the dc conductivity decreased due to the decrease in the crystallinity of samples as shown in PXRD results.

4. Conclusions

Powder XRD results showed that the crystallinity of Zn–Al–NO_3-LDH phase decreased as Zn^{2+}/Al^{3+} molar ratio increases due to the distortion of the hydroxide layers networks by the larger difference in ionic radii of Zn^{2+} and Al^{3+}. Other phases of ZnO and $ZnAl_2O_4$ were formed for LDH with Zn^{2+}/Al^{3+} molar ratio above 2. The prepared LDH samples were macroporous materials due to their volume diameter of pores which was found between 0.28 and 18.86 μm. The characteristic ESR signal of NO_3^- ions with D_{3h} symmetry in the LDH interlayer was obtained due to the interaction between nitrate anions from the interlayer region and a close aluminum nucleus in brucite-like layer of LDH. At Zn^{2+}/Al^{3+} molar ratio of 3 and above, two ESR signals with stronger intensity were produced due to the formation of $ZnAl_2O_4$ and ZnO phases in LDH samples. Thermal diffusivity of LDH samples was found between 2.4 and 3.3 $\times 10^{-7}$ m^2 s^{-1}. The nonlinear behavior of thermal diffusivity against the examined *in situ* temperature is attributed to the presence of water molecules in the LDH below 180°C. The dc conductivity which found from the fit curves of experimental data decreased as Zn^{2+}/Al^{3+} molar ratio increased which may be attributed to the decrease in the crystallinity of samples.

Conflict of Interests

The authors declare that they have no conflict of interests in this work.

Acknowledgments

This study was financed by ERGS/1/11/STG/UPM/02/4 (Postdoctoral Grant). Authors would like to thank Universiti Putra Malaysia (UPM) for supporting this work. A. A. A. Ahmed thanks RMC-UPM and Thamar University, Yemen, for the support.

References

[1] F. Cavani, F. Trifirò, and A. Vaccari, "Hydrotalcite-type anionic clays: preparation, properties and applications," *Catalysis Today*, vol. 11, no. 2, pp. 173–301, 1991.

[2] D. Evans and R. Slade, in *Layered Double Hydroxides*, X. Duan and D. G. Evans, Eds., vol. 119, p. 1, Springer, Berlin, Germany, 2006.

[3] S. Jin, P. H. Fallgren, J. M. Morris, and Q. Chen, "Removal of bacteria and viruses from waters using layered double hydroxide nanocomposites," *Science and Technology of Advanced Materials*, vol. 8, pp. 67–70, 2007.

[4] H. Tamura, J. Chiba, M. Ito, T. Takeda, and S. Kikkawa, "Synthesis and characterization of hydrotalcite-ATP intercalates," *Solid State Ionics*, vol. 172, no. 1–4, pp. 607–609, 2004.

[5] J. Tronto, F. Leroux, M. Dubois, J. F. Borin, C. F. de Oliveira Graeff, and J. B. Valim, "Hyperfine interaction in Zn-Al layered double hydroxides intercalated with conducting polymers," *Journal of Physics and Chemistry of Solids*, vol. 69, no. 5-6, pp. 1079–1083, 2008.

[6] J. Tronto, F. Leroux, M. Dubois et al., "New layered double hydroxides intercalated with substituted pyrroles. 2. 3-(pyrrol-1-yl)-propanoate and 7-(pyrrol-1-yl)-heptanoate LDHs," *Journal of Physics and Chemistry of Solids*, vol. 67, no. 5-6, pp. 973–977, 2006.

[7] K. Bahranowski, R. Dula, F. Kooli, and E. M. Serwicka, "ESR study of the thermal decomposition of V-containing layered double hydroxides," *Colloids and Surfaces A*, vol. 158, no. 1-2, pp. 129–136, 1999.

[8] G. Abellán, E. Coronado, C. J. Gómez-García, C. Martí-Gastaldo, and A. Ribera, "Intercalation of cobalt(II)-tetraphenylporphine tetrasulfonate complex in magnetic NiFe-layered double hydroxide," *Polyhedron*, vol. 52, pp. 216–221, 2013.

[9] A. A. Ali Ahmed, Z. Abidin Talib, and M. Z. B. Hussein, "ESR spectra and thermal diffusivity of ZnAl layered double hydroxide," *Journal of Physics and Chemistry of Solids*, vol. 73, no. 1, pp. 124–128, 2012.

[10] M. M. Sorour, M. M. Saleh, and R. A. Mahmoud, "Thermal conductivity and diffusivity of soil," *International Communications in Heat and Mass Transfer*, vol. 17, no. 2, pp. 189–199, 1990.

[11] W. R. Lindberg, R. R. Thomas, and R. J. Christensen, "Measurements of specific heat, thermal conductivity and thermal diffusivity of Utah tar sands," *Fuel*, vol. 64, no. 1, pp. 80–85, 1985.

[12] K. M. Hinkel, "Estimating seasonal values of thermal diffusivity in thawed and frozen soils using temperature time series," *Cold Regions Science and Technology*, vol. 26, no. 1, pp. 1–15, 1997.

[13] A. A. A. Ahmed, Z. A. Talib, M. Z. bin Hussein, and A. Zakaria, "Zn-Al layered double hydroxide prepared at different molar ratios: preparation, characterization, optical and dielectric properties," *Journal of Solid State Chemistry*, vol. 191, pp. 271–278, 2012.

[14] R. Rojas Delgado, C. P. De Pauli, C. B. Carrasco, and M. J. Avena, "Influence of MII/MIII ratio in surface-charging behavior of Zn-Al layered double hydroxides," *Applied Clay Science*, vol. 40, no. 1–4, pp. 27–37, 2008.

[15] D. Carriazo, M. del Arco, E. García-López et al., "Zn,Al hydrotalcites calcined at different temperatures: preparation, characterization and photocatalytic activity in gas–solid regime," *Journal of Molecular Catalysis A*, vol. 342-343, pp. 83–90, 2011.

[16] T. Ishikawa, K. Matsumoto, K. Kandori, and T. Nakayama, "Synthesis of layered zinc hydroxide chlorides in the presence of Al(III)," *Journal of Solid State Chemistry*, vol. 179, no. 4, pp. 1110–1118, 2006.

[17] K. Dutta, S. Das, and A. Pramanik, "Concomitant synthesis of highly crystalline Zn-Al layered double hydroxide and ZnO: phase interconversion and enhanced photocatalytic activity," *Journal of Colloid and Interface Science*, vol. 366, no. 1, pp. 28–36, 2012.

[18] H. Yan, M. Wei, J. Ma, and X. Duan, "Density functional theory study on the influence of cation ratio on the host layer structure of Zn/Al double hydroxides," *Particuology*, vol. 8, no. 3, pp. 212–220, 2010.

[19] K. S. W. Sing, D. H. Everett, R. A. W. Haul et al., "Reporting physisorption data for gas/solid systems with special reference to the determination of surface area and porosity," *Pure and Applied Chemistry*, vol. 57, no. 4, pp. 603–619, 1985.

[20] M. Shao, J. Han, M. Wei, D. G. Evans, and X. Duan, "The synthesis of hierarchical Zn–Ti layered double hydroxide for efficient visible-light photocatalysis," *Chemical Engineering Journal*, vol. 168, no. 2, pp. 519–524, 2011.

[21] S. I. Bannov and V. A. Nevostruev, "Formation and properties of NO_3^{2-}, NO_3 and ONOO radicals in nitrate-containing matrices," *Radiation Physics and Chemistry*, vol. 68, no. 5, pp. 917–924, 2003.

[22] R. P. Wayne, I. Barnes, P. Biggs et al., "The nitrate radical: physics, chemistry, and the atmosphere," *Atmospheric Environment A*, vol. 25, no. 1, pp. 1–203, 1991.

[23] S. Menon, B. Dhabekar, E. Alagu Raja, S. P. More, T. K. Gundu Rao, and R. K. Kher, "TSL, OSL and ESR studies in $ZnAl_2O_4$:Tb phosphor," *Journal of Luminescence*, vol. 128, no. 10, pp. 1673–1678, 2008.

[24] B. Yu, C. Zhu, F. Gan, and Y. Huang, "Electron spin resonance properties of ZnO microcrystallites," *Materials Letters*, vol. 33, no. 5-6, pp. 247–250, 1998.

[25] R. C. Weast, *Handbook of Chemistry and Physics*, CRC Press, Cleveland, Ohio, USA, 1971.

[26] M. Boutinguiza, F. Lusquiños, J. Pou, R. Soto, F. Quintero, and R. Comesaña, "Thermal properties measurement of slate using laser flash method," *Optics and Laser in Engineering*, vol. 50, no. 5, pp. 727–730, 2012.

[27] H. S. Carslaw and J. C. Jaeger, *Conduction of Heat in Solids*, Clarendon Press, Oxford, UK, 1959.

[28] W. M. M. Yunus, M. Ranjbar, M. Z. B. Hussein, and L. M. Yee, "Thermal diffusivity of zinc-aluminum layered double hydroxide using PVDF photoflash technique," *Journal of Materials Science and Engineering*, vol. 4, p. 7, 2010.

[29] M. H. Sharqawy, "New correlations for seawater and pure water thermal conductivity at different temperatures and salinities," *Desalination*, vol. 313, pp. 97–104, 2013.

[30] X. Cheng, X. Huang, X. Wang, and D. Sun, "Influence of calcination on the adsorptive removal of phosphate by Zn-Al layered double hydroxides from excess sludge liquor," *Journal of Hazardous Materials*, vol. 177, no. 1–3, pp. 516–523, 2010.

[31] M. Z. B. Hussein, T.-Y. Yun-Hin, M. M. B. Tawang, and R. Shahadan, "Thermal degradation of (zinc-aluminium-layered double hydroxide-dioctyl sulphosuccinate) nanocomposite," *Materials Chemistry and Physics*, vol. 74, no. 3, pp. 265–271, 2002.

[32] X. Qu, D. Jia, and S. Lv, "Thermoelectric properties and electronic structure of Al-doped ZnO," *Solid State Communications*, vol. 151, no. 4, pp. 332–336, 2011.

[33] A. K. Jonscher, *Dielectric Relaxation in Solids*, Chelsea Dielectrics Press, London, UK, 1983.